NATIONAL AERONAUTICS AND SPACE ADMINISTRATION

MSC INTERNAL NOTE NO. 69-FM-280

November 4, 1969

APOLLO 12 (MISSION H-1) DISPERSION ANALYSIS

VOLUME IV

DESCENT AND ASCENT DISPERSION ANALYSES

PART 2

LUNAR ASCENT

Landing Analysis Branch

MISSION PLANNING AND ANALYSIS DIVISION

MANNED SPACECRAFT CENTER

HOUSTON, TEXAS

MSC INTERNAL NOTE NO. 69-FM-280

PROJECT APOLLO

APOLLO 12 (MISSION H-1) DISPERSION ANALYSIS
VOLUME IV - DESCENT AND ASCENT DISPERSION ANALYSES
PART 2 - LUNAR ASCENT

By J. V. West
Landing Analysis Branch

November 4, 1969

MISSION PLANNING AND ANALYSIS DIVISION
NATIONAL AERONAUTICS AND SPACE ADMINISTRATION
MANNED SPACECRAFT CENTER
HOUSTON, TEXAS

Approved: Claude A. Graves for
Floyd V. Bennett, Chief
Landing Analysis Branch

Approved:
John P. Mayer, Chief
Mission Planning and Analysis Division

CONTENTS

Section		Page
1.0	SUMMARY	1
2.0	INTRODUCTION	1
3.0	SYMBOLS	2
4.0	DESCRIPTION OF STUDY	3
	4.1 Monte Carlo Technique	3
	4.1.1 Coordinates	3
	4.1.2 Random error initialization	4
	4.1.3 Statistical sampling points	5
	4.1.4 Exclusion of certain cases from the statistics	5
	4.2 Error Sources	6
	4.2.1 Input state vector uncertainties	6
	4.2.2 Inertial sensor errors	7
	4.2.3 Propulsion and mass properties deviations	7
5.0	DISCUSSION OF RESULTS	8
	5.1 Trajectory Dispersion Time Histories	8
	5.2 Trajectory Dispersion Cross Plots	9
	5.3 Dispersions at $\dot{R}$ > 50 fps (end vertical rise)	9
	5.4 Dispersions at Insertion	9
	5.5 Dispersions in LM/CSM Relative Parameters	10
	5.6 Covariance Matrix	10
	5.7 Propellant and ΔV Dispersions	10
6.0	CONCLUSIONS	10
	REFERENCES	36

TABLES

Table		Page
I	INITIAL CSM COVARIANCE MATRIX	12
II	INITIAL LM STATE VECTOR UNCERTAINTIES	13
III	APS PERFORMANCE DISPERSIONS	13
IV	INITIAL c.g. DISPERSIONS	14
V	APS ENGINE LOCATION AND THRUST DIRECTION DISPERSIONS	14
VI	INPUT WEIGHT DISPERSIONS	15
VII	PGNCS IMU DEVIATIONS	16
VIII	AGS SENSOR DEVIATIONS	16
IX	DISPERSIONS IN ACTUAL INSERTION PARAMETERS	17
X	DISPERSIONS IN PGNCS TARGET PARAMETERS AT INSERTION	18
XI	DISPERSIONS IN ORBIT PARAMETERS	18
XII	DISPERSIONS IN LM/CSM RELATIVE PARAMETERS AT INSERTION	19
XIII	ΔV DISPERSIONS	19
XIV	APS OXIDIZER DISPERSIONS	20
XV	APS FUEL DISPERSIONS	20
XVI	APS PROPELLANT DISPERSIONS	20
XVII	TWENTY-FOUR-BY-24 COVARIANCE MATRIX	21
	(a) Format	21
	(b) Column 1	22
	(c) Column 2	23
	(d) Column 3	24
	(e) Column 4	25

FIGURES

Figure		Page
1	Dispersions in altitude	26
2	Altitude rate dispersions	27
3	Actual out-of-plane distance deviations	28
4	Dispersions in the angle at center of moon between landing site and LM	29
5	Dispersions in actual inertial velocity	30
6	Actual dispersions in pitch from local vertical	31
7	Terrain clearance over highest elevations near lunar ascent groundtrack (site 7)	32
8	Inertial velocity versus flight-path angle	33
9	Altitude versus altitude rate. (Actual)	34
10	3σ position ellipsoid at t_{IG} + 460 seconds	35

APOLLO 12 (MISSION H-1) DISPERSION ANALYSIS

VOLUME IV - DESCENT AND ASCENT DISPERSION ANALYSES

PART 2 - LUNAR ASCENT

By J. V. West

1.0 SUMMARY

A 100-case Monte Carlo analysis of the lunar module (LM) ascent phase of Apollo 12 (Mission H-1) was performed, and the results are presented in statistical tables, insertion ellipsoids, time histories, cross plots, and covariance matrices.

There were no violations of ascent mission or system constraints. The mean time of powered flight is 431 seconds with a 3σ dispersion of ±16 seconds. The 3σ position ellipsoid at 460 seconds after lift-off had radial, down-range, and cross-range semiaxis dimensions of 0.8 n. mi., 11.6 n. mi., and 2.9 n. mi., respectively. At insertion, the 3σ dispersion in the magnitude of the actual velocity vector is 13 fps; and, in the corresponding estimated vector onboard the spacecraft, the dispersion is 8 fps. The 3σ dispersion in the wedge angle between the command/service module (CSM) and LM orbits is 0.3°.

2.0 INTRODUCTION

The results of dispersion analyses for the nominal launch and powered ascent from the lunar surface are presented and described in this document. Initial CSM state vector uncertainties described in reference 1 and LM state uncertainties described in reference 2 were used as inputs for this study. Initial state vectors were taken from reference 3, and a gravity model based on Apollo 8 navigation experience (Boeing R2 lunar potential model, reference 4) was used for state vector integration.

In addition to the CSM and landing site uncertainties, deviations were applied to the propulsion systems (refs. 5 and 6), inertial measurement unit (IMU) (ref. 7), and mass properties (ref. 8). The abort guidance system (AGS) in the followup mode, and its inertial sensor errors (ref. 7) were also dispersed.

3.0 SYMBOLS

AGS	abort guidance system
APS	ascent propulsion system
CANT	engine gimbal angle about Y-body axis, deg
c.g.	center of gravity
CSM	command/service module
DAP	digital autopilot
FDAI	Flight Director Attitude Indicator
h	altitude, ft
$\dot{h}$	altitude rate, fps
IMU	inertial measurement unit
I_{sp}	specific impulse
LAB	Landing Analysis Branch
LGC	lunar module guidance computer
LM	lunar module
LOS	line of sight
PGNCS	primary guidance and navigation control subsystem
PSI	engine gimbal angle about Z-body axis, deg
RCS	reaction control system
$\dot{R}$	radial rate, fps
T/W	thrust-to-weight ratio
t_{IG}	time of ignition (lunar lift-off)
U, V, W	local vertical coordinate system in which covariance matrices are computed, ft

XB, YB, ZB	location of APS engine in X, Y, Z body station coordinates
$X_{c.g.}$, $Y_{c.g.}$, $Z_{c.g.}$	center of gravity in X, Y, Z body station coordinates, in.
γ	flight-path angle, deg

4.0 DESCRIPTION OF STUDY

The techniques used to obtain dispersion data for the nominal LM ascent from the lunar surface are described in this section. These techniques are the same as those described in reference 9 except that no linear analysis was performed and a modified IMU error model has been incorporated in the DAMP program referred to in section 4.1. Under the control of the PGNCS guidance, the LM ascent trajectory consists of a vertical rise from the lunar surface until the altitude rate exceeds 50 fps, at which point the vehicle pitches over approximately 52° from the vertical and ascends to a point (determined by velocity) at which the APS is cut off (ref. 10). A 100-case Monte Carlo simulation of the LM ascent trajectory is the source of the dispersion data presented in this document.

4.1 Monte Carlo Technique

The basic elements of the Monte Carlo method of dispersion analysis will be described in this section. Data for the 100-case Monte Carlo dispersion analysis were generated by the LAB DAMP program which performed the Monte Carlo simulations and the TRW PROC program which was used for additional statistical processing. State vector uncertainties, (refs. 1 and 2), systems dispersions (refs. 5, 6, and 7), and mass properties deviations (ref. 8) were applied to the Monte Carlo simulation of the ascent trajectory. These initial deviations are shown in tables I through VIII, and initial state vectors were taken from reference 3.

4.1.1 Coordinates.- Covariance matrices were computed in a local vertical U, V, W coordinate system which is defined below.

$$\underline{U} = \frac{\underline{r}}{|\underline{r}|}, \text{ vertical}$$

$$\underline{V} = \underline{W} \times \underline{U}, \text{ down range}$$

$$\underline{W} = \frac{\underline{m}}{|\underline{m}|}, \text{ cross range}$$

where

$\underline{r}$ = position vector

$\underline{m}$ = momentum vector ($\underline{r} \times \underline{v}$)

$\underline{v}$ = vecloity vector

The U, V, W system used for the landing site covariance matrix was fixed at the nominal landing site, and the coordinates for the matrices produced during the powered ascent were fixed on the nominal trajectory at the particular point of interest (e.g., t_{IG} plus 460 sec or at insertion).

Local vertical velocities ($\dot{R}$, $\dot{Y}$, $\dot{Z}$) used by the ascent guidance to compute the desired thrust direction are computed in a system defined below.

$$\underline{R} = \frac{\underline{r}}{|\underline{r}|}, \text{ vertical}$$

$$\underline{Y} = \underline{Z} \times \underline{R}, \text{ cross range}$$

$$\underline{Z} = \frac{\underline{r} \times \underline{Q}}{|\underline{r} \times \underline{Q}|}, \text{ down range}$$

where

$\underline{r}$ = LM position vector

$\underline{v}$ = LM velocity vector

$\underline{Q}$ = CSM negative momentum vector ($\underline{v} \times \underline{r}$)

It is important to note that both the LM and CSM state vectors were used in the LGC to form this coordinate system; therefore, the uncertainties in both state vectors contribute to powered ascent dispersions. Actual and estimated velocities presented in table IX are in this coordinate system.

4.1.2 Random error initialization.- For each Monte Carlo run, a random number was chosen for each dispersed system parameter. The random number generation scheme shaped the statistical distribution of the chosen numbers such that their variance was 1 and their mean value was zero. These Gaussianly distributed random numbers were

multiplied by the 1σ deviations of the parameters to be dispersed, and the products were added to the nominal values. A computer simulation of the powered ascent was then run, and these randomly modified values were used to define the input conditions. This process was repeated 100 times, and a new set of random numbers was used for each simulation. Note that all initial dispersions were assumed to fit a normal distribution. The sampling of covariance matrices is described in reference 11.

4.1.3 Statistical sampling points.- At six points along the LM powered ascent trajectory, various trajectory and system parameters were sampled and retained during the 100 simulation runs. Then these data were processed statistically by the DAMP and PROC programs. Covariance matrices, standard deviations, and cumulative distributions for parameters such as perilune altitude and radial rate was computed.

A U, V, W coordinate system was defined and fixed on the nominal trajectory at each of the six points where statistical samples were taken. During each dispersed run, the actual and the estimated state vectors were transformed into the nominal U, V, W system; then the differences between the actual and nominal and the estimated and the actual state were computed. After statistical processing, these differences were used to determine the actual and estimated covariance matrices. The six points at which sampling took place are defined below.

a. $\dot{R} > 50$ fps (end of vertical rise phase)

b. t_{IG} plus 120 seconds

c. t_{IG} plus 240 seconds

d. t_{IG} plus 360 seconds

e. Insertion

f. t_{IG} plus 460 seconds

Except for the samples taken when $\dot{R}$ first exceeded 50 fps and at insertion, all samples were time fixed. Sampling at t_{IG} plus 460 seconds was necessary to obtain time-fixed covariance matrices after burnout for the initialization of a rendezvous dispersion analysis. Insertion always occurred before that time, and Encke integration was used to advance the state vector to t_{IG} plus 460 seconds.

4.1.4 Exclusion of certain cases from the statistics.- Criteria used to exclude Monte Carlo simulation cases from the final statistics

were included in the program. These constraints were as follows.

a. Perilune altitude above the radius of the landing site less than 30 000 feet at insertion

b. Wedge angle greater than 2° at insertion

c. APS propellant depletion

The orbital limits were chosen because flight controller commanded switchover to AGS guidance would occur if the limits were approached and this switchover could not be simulated. If these constraints are violated, the results will be included in mission success probability. In this study, no cases violated these contraints.

4.2 Error Sources

The initial dispersions of trajectory and vehicle parameters which were used as input for these analyses are described below.

4.2.1 Input state vector uncertainties.- Because both the CSM and the LM state vectors are used by the AGC to compute insertion targets, covariance matrices for both vehicles must be considered in an ascent dispersion analysis. The definition of and format for a six-by-six state vector covariance matrix in the U, V, W system is shown below.

$$\left[\sigma\right] = \frac{1}{N-1}\left[\sum_{i=1}^{N} X_i X_i^T - \frac{1}{N}\sum_{i=1}^{N} X_i \left(\sum_{i=1}^{N} X_i\right)^T\right]$$

where

X_i = ith U, V, W, $\dot{U}$, $\dot{V}$, $\dot{W}$ state vector

N = number of state vectors

$[\sigma]$ = covariance matrix whose format is as follows

$$\begin{matrix} \sigma_{UU} & \sigma_{UV} & \sigma_{UW} & \sigma_{U\dot{U}} & \sigma_{U\dot{V}} & \sigma_{U\dot{W}} \\ & \sigma_{VV} & \sigma_{VW} & \sigma_{V\dot{U}} & \sigma_{V\dot{V}} & \sigma_{V\dot{W}} \\ & & \sigma_{WW} & \sigma_{W\dot{U}} & \sigma_{W\dot{V}} & \sigma_{W\dot{W}} \\ \text{(symmetrical)} & & & \sigma_{\dot{U}\dot{U}} & \sigma_{\dot{U}\dot{V}} & \sigma_{\dot{U}\dot{W}} \\ & & & & \sigma_{\dot{V}\dot{V}} & \sigma_{\dot{V}\dot{W}} \\ & & & & & \sigma_{\dot{W}\dot{W}} \end{matrix}$$

For this study, it was assumed that initial deviations of the actual state vector from the nominal could be considered to be zero because the actual landing site and CSM position will be determined by various sighting and tracking techniques and updated information will be sent to the CMC and LGC before launch. Therefore, for initialization of each Monte Carlo run, only uncertainties in the estimated state vectors were considered. Input covariance matrices are shown in tables I and II.

4.2.2 Inertial sensor errors.- The PGNCS IMU errors and deviations are listed in table VII. The IMU platform was assumed to be alined through the estimated position vector 15 minutes before lift-off. An AGS estimated state vector was computed with the AGS in the followup mode (alined to PGNCS 5 min before ignition, state updated during flight) during this dispersion analysis. The AGS gyro and accelerometer errors were randomized and included in the simulation. The errors and deviations used are shown in table VIII, and the basic source for both the PGNCS and AGS data was reference 6.

4.2.3 Propulsion and mass properties deviations.- Because the ascent engine is not gimballed, it cannot be used for steering purposes, and the thrust vector must be controlled by pointing the entire ascent stage in the desired direction; RCS jets are used for this purpose. If the thrust vector does not pass through the center of gravity, there will be a rotational moment about the body axes caused by the APS thrust which must be balanced by RCS thrust. The DAP is programmed to use (whenever possible) only RCS jets that thrust along the positive X-body axis so that the thrusting required to balance the APS moments adds to the APS thrust. These designed characteristics make the powered ascent phase unusually sensitive to the c.g. location and thrust direction.

To include the effects discussed above and the APS performance variations in this dispersion analysis, the following parameters were randomly dispersed.

a. Inert weight

b. APS oxider weight

c. APS fuel weight

d. RCS oxidizer weight

e. RCS fuel weight

f. X, Y, Z c.g. location

g. Y, Z engine mounting location

h. APS thrust direction in XZ body plane

i. APS thrust direction in XY body plane

j. APS thrust

k. APS I_{sp}

l. APS mixture ratio

The nominal values and their deviations are shown in tables III, IV, V, and VI. The sources for these data and for the mathematical model used to compute the unbalanced moments and RCS thrust were references 5 and 6.

5.0 DISCUSSION OF RESULTS

Dispersion data which result from the analyses described in this document are presented in the form of time histories, cross plots, position ellipsoids, covariance matrices, and tables.

5.1 Trajectory Dispersion Time Histories

Plots of various trajectory parameters versus time are presented in figures 1 through 6. A dispersion cross centered on the nominal insertion point is shown, and it indicates the time deviation as well

as the time-fixed dispersion of the parameter of interest. The dispersion boundaries were not extended to the insertion crosses to avoid ambiguous interpretation of the data.

5.2 Trajectory Dispersion Cross Plots

Cross plots of dispersed parameters such as altitude versus altitude rate and flight-path angle γ versus velocity V are presented in figures 7, 8, and 9. Three-sigma dispersion crosses are shown in the figures at the times when one-dimensional time-fixed dispersions were computed.

5.3 Dispersions at $\dot{R} > 50$ fps (end vertical rise)

The uncertainty in the T/W ratio causes some of the Monte Carlo cases to simulate a 10-second vertical rise time instead of a 12-second rise time simulated by other cases. If the vertical rise time extends one computer cycle (2 sec) past the nominal rise time of 10 seconds, the required ΔV increases by approximately 12 fps, and the altitude at the beginning of pitchover changes from approximately 250 feet to 350 feet. The 10.3-second mean duration of the vertical rise phase computed by the Monte Carlo study implies that in approximately 15 percent of the 100 cases 12-second vertical rise times were simulated.

5.4 Dispersions at Insertion

At insertion, the dispersions which are of greatest interest include the burn time, position ellipsoid, guidance targets, and orbital parameters. The mean burn time was 432 seconds with a 3σ deviation of 15.9 seconds. This large burn time deviation resulted from APS, weight, and c.g. dispersions. The dispersions in several parameters at insertion are given in table IX. The dispersions in the velocity components appear large with respect to the dispersion in the magnitude of the total insertion velocity because errors such as platform misalinement change the direction of the velocity vector but do not change the magnitude. A comparison of the desired guidance targets with the nominal, mean, and 3σ dispersion values for the PGNCS estimated state vector is shown in table X. The relatively large down-range velocity residual in the estimated state vector is caused by thrust tailoff uncertainties and can be removed by a trim maneuver. The uncertainty in the magnitude of the actual velocity vector is 13 fps and the dispersion in the PGNCS estimated velocity vector is 8 fps.

The 3σ three-dimensional ellipsoid of actual position uncertainty is presented in figure 10. Data for figure 10 were computed from the results

of a time-fixed sampling of position vectors taken 460 seconds after lift-off. The down-range component is larger than the corresponding one for Apollo 11 which reflects the increase in thrust dispersion given in reference 5.

A summary of dispersions in the parameters of the orbit achieved by powered ascent is given in table XI. Perilune and apolune of the orbit achieved at insertion had 3σ dispersions of 2040 feet and 37 800 feet, respectively. Other 3σ dispersions were 9° for the true anomaly and 0.3° for the wedge angle.

5.5 Dispersions in LM/CSM Relative Parameters

Dispersions of LM to CSM relative parameters are shown in table XII. The 12-fps dispersion in range rate gives some indication of the rendezvous radar accuracy at insertion. The range of 260n. mi. is within rendezvous radar capability.

5.6 Covariance Matrix

Covariance and cross covariance terms for the CSM estimated, LM actual, LM estimated, and AGS estimated state vector uncertainties are shown in a 24- by-24 covariance matrix presented in table XVII. The format of the matrix is also presented in table XVII. This covariance matrix was computed in the nominal U, V, W coordinate system described in section 4.1.1 from 100 simulation samples taken 460 seconds after lift-off.

5.7 Propellant and ΔV Dispersions

In tables XIV, XV, and XVI, summaries are presented of the loaded, required, total remaining, and usable remaining propellant with 3σ dispersions for APS oxidizer, fuel, and propellant. The tables include the usable remaining propellant because the required propellant weights do not reflect mixture ratio uncertainties. None of the cases in the 100-sample Monte Carlo simulation burned to depletion. The ΔV information for the total powered ascent is presented in table XIII.

6.0 CONCLUSIONS

None of the 100 Monte Carlo simulations violated mission or system constraints, and no case burned the usable propellants to depletion.

The 3σ dimensions of the position ellipsoid 460 seconds after lift-off are 0.8 n. mi. in the radial direction, 11.6 n. mi. in the downrange direction, and 2.9 n. mi. in the crossrange direction. The 3σ magnitude of the true velocity dispersion at insertion is 13 fps, and the uncertainty in the PGNCS estimate of the 3σ residual velocity magnitude is 8 fps. The 3σ dispersions in perilune and apolune after thrust termination are approximately 0.34 n. mi. and 6.2 n. mi., respectively.

TABLE I.- INITIAL CSM COVARIANCE MATRIX

U	V	W	$\dot{U}$	$\dot{V}$	$\dot{W}$
.2578471+007	-.9534960+006	.1010955+002	.7995407+003	-.2271524+004	.5389155-001
-.1391047+000	.1822182+008	.1560969+004	-.1606012+005	.6368071+003	.9651214+001
.3455258-005	.2006911-003	.3320020+007	-.1383364+001	-.1392494-001	.1394266+005
.1248487+000	-.9433598+000	-.1903666-003	.1590564+002	-.5242362+000	-.8554116-002
-.9988179+000	.1053325+000	-.5396017-005	-.9281146-001	.2005855+001	-.7889563-004
.3617362-005	.2436905-003	.8247605+000	-.2311809-003	-.6004206-005	.8607858+002

TABLE II.- INITIAL LM STATE VECTOR UNCERTAINTIES

	U	V	W	$\dot{U}$	$\dot{V}$	$\dot{W}$
U	0	0	0	0	0	0
V		$1.6X10^7$	0	0	0	0
W			$1.6X10^7$	0	0	0
$\dot{U}$		(symmetric)		0	0	0
$\dot{V}$					0	0
$\dot{W}$						0

TABLE III.- APS PERFORMANCE DISPERSIONS

Parameter	Nominal	3σ
Thrust, lb	[a] 3470	[b] 107.4
Isp, sec	309.5	3.639
Oxidizer/fuel, n.d.	1.605	.0282

[a] Integrated ave.; actual thrust computed by polynomial fit to data in ref. 5.

[b] Actual thrust dispersion includes correlation with Isp dispersion as suggested in ref. 5.

TABLE IV.- INITIAL c.g. DISPERSIONS

Vehicle body axis	Initial c.g. location[a], in.[b]	3σ, in.[b]
X	243.4	0.7
Y	.10	0.4
Z	2.5	0.4

[a]Actual c.g. location was programed as a function of weight (ref. 8).

[b]Body station coordinates.

TABLE V.- APS ENGINE LOCATION AND THRUST DIRECTION DISPERSIONS

	Nominal	3σ	Units
XB	232.96	0.7	inches[a]
YB	0.0	0.4	inches
ZB	3.75	0.4	inches
CANT	-1.5	1.0	degrees
PSI	0.0	1.0	degrees

[a]Body station coordinates.

TABLE VI.- INPUT WEIGHT DISPERSIONS

Weight component	Nominal, lb	3σ, lb
Available APS oxidizer	3189.7	8
Available APS fuel	1997.4	5
Available RCS oxidizer	391.8	3.3
Available RCS fuel	200.6	1.7
Nonpropulsive weight	4954.8	25.0
Total weight	10 734.3	26.9

TABLE VII.- PGNCS IMU DEVIATIONS

Parameter	3σ
Platform misalinement, rad	0.00115
Gyro drift (powered flight), rad/sec	.00000112
Gyro drift (surface), rad/sec	.000000489
Accelerometer bias, ft/sec^2	.00656
Accelerometer scale factor, ppm	300
Gyro spin reference axis g-sensitive drift, rad/fps	0.0000000339
Gyro input axis g-sensitive drift, drift, rad/fps	0.0000000542

TABLE VIII.- AGS SENSOR DEVIATIONS

Parameter	3σ
Misalinement (lunar surface), rad	0.0015
Gyro drift (ascent), rad/sec	.00000952
Gyro drift (surface), rad/sec	.00000728
Gyro scale factor, ppm	551
Accelerometer bias, ft/sec^2	.01858
Accelerometer scale factor, ppm	900
Accelerometer misalinement (x only), rad	.00063

TABLE IX.- DISPERSIONS IN ACTUAL INSERTION PARAMETERS

Parameter	Nominal	Mean	±3σ	Percentile	
				First	Ninety-ninth
Altitude, ft	60 016	60 074	3180	57 886	62 602
Out-of-plane distance, ft	0	-448	13 734	-11 954	12 861
Down-range distance, n. mi.	165	165	5.7	164.8	165.5
Radial rate, fps	31.5	31.6	15.6	20.8	43.5
Out-of-plane velocity, fps	0	0	[a]30.3	[a]-19.9	[a]22.5
Down-range velocity, fps	5535.4	5535.2	12.3	5527.7	5541.8
Total velocity, fps	5535.9	5535.3	13.0	[b]	[b]
Burn arc, deg	10.07	10.07	.345	[b]	[b]
Burn time, sec	431.5	431.1	15.9	419.9	442.6
Outer gimbal angle (yaw), deg	0	0	.3	-.2	.3
Inner gimbal angle (pitch), deg	-103.0	-103.0	1.0	-103.5	-102.1
Middle gimbal angle, (roll), deg	0	.1	1.4	-1.0	1.3

[a]Includes CSM uncertainty.

[b]Not available.

TABLE X.- DISPERSIONS IN PGNCS TARGET PARAMETERS AT INSERTION

Parameter	Nominal	Mean	±3σ	Percentile	
				First	Ninety-ninth
Altitude, ft	60 116	60 106	73.8	60 072	60 148
Out-of-plane distance, ft	0	0	.1	-.05	.09
Radial rate, fps	32.1	32.1	.1	32.0	32.2
Out-of-plane velocity, fps	0	0	0	-.03	.05
Down-range velocity fps	5535.5	5535.5	8.4	5528.4	5542.9

TABLE XI.- DISPERSIONS IN ORBIT PARAMETERS

Parameter	Nominal	Mean	±3σ	Percentile	
				First	Ninety-ninth
Perilune altitude, ft	55 015	54 864	2040	52 783	55 842
Apolune altitude, n. mi.	46.5	46.4	6.2	41.2	51.5
True anomaly, deg	17.38	17.54	8.97	11.28	25.44
Wedge angle, deg	0	0	.3	-.29	0.297

TABLE XII.- DISPERSIONS IN LM/CSM RELATIVE PARAMETERS AT INSERTION

Parameter	Nominal	Mean	±3σ	Percentile	
				First	Ninety-ninth
Range, n. mi.	260	260	8.5	253	267
Range rate, fps	455	455	12.1	443	463
Phase angle, deg	-15.1	-15.1	.52	-15.5	-14.7
Elevation angle (LOS to LM YZ-body axis plane), deg	83.8	83.8	.13	83.0	85.0

TABLE XIII.- ΔV DISPERSIONS

Parameter	Nominal	Mean	±3σ	Percentile	
				First	Ninety-ninth
ΔV required at I_{sp} = 309.1 ± 3.7 sec, fps	6050	6050	30.9	6036	6087
ΔV remaining at I_{sp} = 309.4 ± 3.9 sec, fps	494	486	101.1	400	569

TABLE XIV.- APS OXIDIZER DISPERSIONS

APS oxidizer parameter	Nominal	Mean	±3σ	Percentile	
				First	Ninety ninth
Loaded, lb	3223.9	3223.9	8	a	a
Required, lb	3016	3018	42.7	2975	3040
Remaining, lb	207.9	205.9	36	a	a
Usable remaining, lb	174	171	33	a	a

[a]Not available.

TABLE XV.- APS FUEL DISPERSIONS

APS fuel parameter	Nominal	Mean	±3σ	Percentile	
				First	Ninety ninth
Loaded, lb	2012.1	2012.1	5	a	a
Required, lb	1873	1874	36.2	1846	1900
Remaining, lb	139.1	138.1	31	a	a
Usable remaining, lb	109	107	21.6	a	a

[a]Not available.

TABLE XVI.- APS PROPELLANT DISPERSIONS

APS propellant parameter	Nominal	Mean	±3σ
Loaded, lb	5236	5236	9.5
Required, lb	4889	4892	52.8
Remaining, lb	347	344	67
Usable remaining, lb	283	278	55.8

TABLE XVII.- TWENTY FOUR-BY-24 COVARIANCE MATRIX

(a) Format

$\begin{pmatrix} \text{CSM} \\ \text{EST} \end{pmatrix}$	$\begin{pmatrix} \text{CSM} \\ \text{EST} \end{pmatrix} \times \begin{pmatrix} \text{LM} \\ \text{ACT} \end{pmatrix}$	$\begin{pmatrix} \text{CSM} \\ \text{EST} \end{pmatrix} \times \begin{pmatrix} \text{LM} \\ \text{EST} \end{pmatrix}$	$\begin{pmatrix} \text{CSM} \\ \text{EST} \end{pmatrix} \times \begin{pmatrix} \text{AGS} \\ \text{EST} \end{pmatrix}$
$\left[\begin{pmatrix} \text{CSM} \\ \text{EST} \end{pmatrix} \times \begin{pmatrix} \text{LM} \\ \text{ACT} \end{pmatrix}\right]^T$	$\begin{pmatrix} \text{LM} \\ \text{ACT} \end{pmatrix}$	$\begin{pmatrix} \text{LM} \\ \text{ACT} \end{pmatrix} \times \begin{pmatrix} \text{LM} \\ \text{EST} \end{pmatrix}$	$\begin{pmatrix} \text{LM} \\ \text{ACT} \end{pmatrix} \times \begin{pmatrix} \text{AGS} \\ \text{EST} \end{pmatrix}$
$\left[\begin{pmatrix} \text{CSM} \\ \text{EST} \end{pmatrix} \times \begin{pmatrix} \text{LM} \\ \text{EST} \end{pmatrix}\right]^T$	$\left[\begin{pmatrix} \text{LM} \\ \text{ACT} \end{pmatrix} \times \begin{pmatrix} \text{LM} \\ \text{EST} \end{pmatrix}\right]^T$	$\begin{pmatrix} \text{LM} \\ \text{EST} \end{pmatrix}$	$\begin{pmatrix} \text{LM} \\ \text{EST} \end{pmatrix} \times \begin{pmatrix} \text{AGS} \\ \text{EST} \end{pmatrix}$
$\left[\begin{pmatrix} \text{CSM} \\ \text{EST} \end{pmatrix} \times \begin{pmatrix} \text{AGS} \\ \text{EST} \end{pmatrix}\right]^T$	$\left[\begin{pmatrix} \text{LM} \\ \text{ACT} \end{pmatrix} \times \begin{pmatrix} \text{AGS} \\ \text{EST} \end{pmatrix}\right]^T$	$\left[\begin{pmatrix} \text{LM} \\ \text{EST} \end{pmatrix} \times \begin{pmatrix} \text{AGS} \\ \text{EST} \end{pmatrix}\right]^T$	$\begin{pmatrix} \text{AGS} \\ \text{EST} \end{pmatrix}$
TABLE XVII (b)	TABLE XVII (c)	TABLE XVII (d)	TABLE XVII (e)

TABLE XVII.- TWENTY FOUR-BY-24 COVARIANCE MATRIX - Continued

(b) Column 1

(CSM estimated

2.3769480+006	-2.0803749+006	-1.4181082+005	1.7541008+003	-2.1016785+003	-1.8543370+002
-2.0803749+006	1.9287023+007	-4.8155007+005	-1.5538251+004	1.6549227+003	-1.0593355+003
-1.4181082+005	-4.8155007+005	2.7829558+007	-5.5069883+002	1.5652355+002	3.7660516+004
1.7541008+003	-1.5538251+004	-5.5069883+002	1.4746433+001	-1.3847975+000	-5.3056131-001
-2.1016785+003	1.6549227+003	1.5652355+002	-1.3847975+000	1.8626572+000	2.1380134-001
-1.8543370+002	-1.0593355+003	3.7660516+004	-5.3056131-001	2.1380134-001	5.4155865+001

(CSM estimated × LM actual)^T

2.3767133+005	6.0264662+003	8.8332718+005	5.1556307+001	-2.1137782+002	1.0486756+003
2.8576677+006	-1.1426392+007	1.3837654+007	7.7435030+003	-2.5191119+003	1.7526662+004
-8.3859363+005	1.5631289+006	1.4502535+007	-1.5360153+003	7.1513101+002	1.8699040+004
-1.9108703+003	1.1042051+004	-1.0148655+004	-7.0843533+000	1.6822138+000	-1.3399188+001
-5.7321455+002	-1.3345266+003	-2.6776754+003	1.5579772+000	5.2639744-001	-4.4199359+000
9.4255464+002	-3.3812575+003	4.7074131+004	8.6845839-001	-7.0553242-001	6.7371079+001

(CSM estimated × LM estimated)^T

-2.0235748+005	-1.3267149+005	-7.3625433+005	3.2018442+001	1.8007508+002	-8.5900995+002
2.0678455+005	-1.3741471+006	-3.5949641+006	4.4289548+002	-1.8173527+002	-4.7925733+003
7.6093169+005	-1.6943479+006	5.6382204+005	1.1589077+003	-6.3176295+002	8.0321846+002
-9.6178980+002	9.6549288+002	7.1687821+002	-5.9512834-001	8.4945483-001	1.6901568+000
5.6799026+002	1.3683955+003	2.6228897+003	-1.5786397+000	-5.2177824-001	4.3521088+000
-1.1582118+003	2.1931083+003	-2.7634037+003	-1.5179871+000	9.5371958-001	-4.2176114+000

(CSM estimated × AGS estimated)^T

-6.9957568+004	-9.5699727+005	-6.2087931+005	5.6178433+002	7.0539000+001	-8.2038601+002
2.7528890+005	-1.0264666+006	-4.1795957+006	8.5716246+002	-2.3517661+002	-5.7315342+003
6.3465873+005	-2.0687111+006	1.8876403+006	1.3076676+003	-5.1084665+002	2.7421547+003
-6.0000375+002	-2.6011363+003	3.1056546+002	1.5018649+000	5.6416691-001	5.0210128-001
8.0188231+002	9.4664076+001	5.1371637+002	2.2940071-001	-6.9847121-001	9.4378198-001
-2.2575415+003	3.1078390+002	3.2819087+003	-7.8104841-001	1.9757498+000	4.7537240+000

TABLE XVII.- TWENTY FOUR-BY-24 COVARIANCE MATRIX - Continued

(c) Column 2

(CSM estimated × LM actual)

LM actual

1.3685542+006	4.0959856+006	-2.2953936+005	1.9334446+003	-1.4480745+003	1.9911702+003
4.0959856+006	3.9327644+008	8.8257714+006	-3.3571572+005	7.3003318+003	2.4211554+004
-2.2953936+005	8.8257714+006	2.2173899+007	-9.9187794+003	-2.1732923+003	1.8879463+004
1.9334446+003	-3.3571572+005	-9.9187794+003	3.3545623+002	-1.1782721+001	-1.6023324+001
-1.4480745+003	7.3003318+003	-2.1732923+003	-1.1782721+001	9.9357197+000	-6.3213268+000
1.9911702+003	2.4211554+004	1.8879463+004	-1.6023324+001	-6.3213268+000	1.0238204+002

(LM actual × LM estimated)^T

-1.3240953+006	-2.8473119+005	3.4112981+005	-5.4627328+003	1.4776338+003	-1.7414955+003
-2.2075474+006	-1.7137620+006	-2.6243608+006	-8.4472608+003	3.7540978+003	-7.9389790+003
7.5032106+005	-1.0232664+006	-1.4077551+007	4.3641095+003	9.4675685+002	5.5947534+003
-3.6288462+003	-2.3619257+003	4.2243601+003	-1.3330428+001	1.2938228+000	1.1074444+000
1.4129645+003	-8.5051359+003	2.1345802+003	1.2789204+001	-9.9406884+000	6.2221778+000
-7.2936387+002	-3.3978254+003	3.2280308+003	2.2671110-001	1.2650857+000	-2.3743820+001

(LM actual × AGS estimated)^T

-7.2688864+005	-2.4374260+006	-5.1390919+005	-7.3950282+002	1.4507548+003	-1.0015859+003
-2.2023682+006	1.0688203+005	-3.2062447+006	-9.8290357+003	5.3045581+003	-8.8129579+003
9.0841295+005	2.8971436+006	-1.2625882+007	1.1740621+003	4.5639519+002	1.1304805+004
-1.2142777+003	-1.7469508+004	-2.5289360+002	1.2089627+001	1.0933498+000	3.2925798+000
1.4839689+003	-5.1571678+002	1.0041346+002	6.8422196+000	-3.6721893+000	3.0882166+000
-2.7545461+002	1.5021490+004	1.0502688+004	-1.6014276+001	-8.2535118-001	1.0701164+000

TABLE XVII.- TWENTY FOUR-BY-24 COVARIANCE MATRIX - Continued

(d) Column 3

(CSM estimated × LM estimated)

(LM actual × LM estimated)

LM estimated

1.3206746+006	2.1965659+006	-7.8016287+005	3.6042428+003	-1.4539747+003	7.0429174+002
2.1965659+006	1.2133017+007	6.5107281+005	-1.6682324+003	-3.0333606+003	2.2921894+003
-7.8016287+005	6.5107281+005	1.4384771+007	-4.0414774+003	-9.3975292+002	-4.5993456+003
3.6042428+003	-1.6682324+003	-4.0414774+003	1.7143686+001	-1.2912552+000	7.3994547-001
-1.4539747+003	-3.0333606+003	-9.3975292+002	-1.2912552+000	9.9532995+000	-1.2466780+000
7.0429174+002	2.2921894+003	-4.5993456+003	7.3994547-001	-1.2466780+000	1.8846135+001

(LM estimated × AGS estimated)^T

6.9608244+005	2.0547777+006	1.6931777+005	1.0326347+003	-1.4299669+003	3.5420450+001
2.1989888+006	1.2056655+007	9.5743221+005	-1.9212632+003	-5.1951147+003	2.0885939+003
-8.9814099+005	-2.2677792+005	1.3608199+007	-3.6659092+003	-4.7505152+002	-8.0571258+003
1.0074481+003	-2.0941669+003	3.9261695+002	6.2729236+000	-1.0903025+000	-2.7070353+000
-1.4880258+003	-4.1631727+003	1.0444324+002	-2.3284169+000	3.6343487+000	-2.0210286+000
4.4271640+002	-1.7124871+003	-8.8293627+003	3.6436160+000	7.2789927-001	4.4349297+000

TABLE XVII.- TWENTY FOUR-BY-24 COVARIANCE MATRIX - Concluded

(e) Column 4

(CSM estimated × AGS estimated)

(LM actual × AGS estimated)

(LM estimated × AGS estimated)

AGS estimated

1.8163620+006	1.5737965+006	1.7701776+005	7.3357176+003	-2.9970312+003	3.6259163+002
1.5737965+006	1.3044443+007	1.7976877+004	-5.4094756+003	-1.5454624+003	-2.4912990+003
1.7701776+005	1.7976877+004	1.5445573+007	1.4660809+003	3.8229336+002	1.1477655+003
7.3357176+003	-5.4094756+003	1.4660809+003	4.2778770+001	-1.2542926+001	3.6028554+000
-2.9970312+003	-1.5454624+003	3.8229336+002	-1.2542926+001	1.4013473+001	-1.9342707+000
3.6259163+002	-2.4912990+003	1.1477655+003	3.6028554+000	-1.9342707+000	5.6251699+001

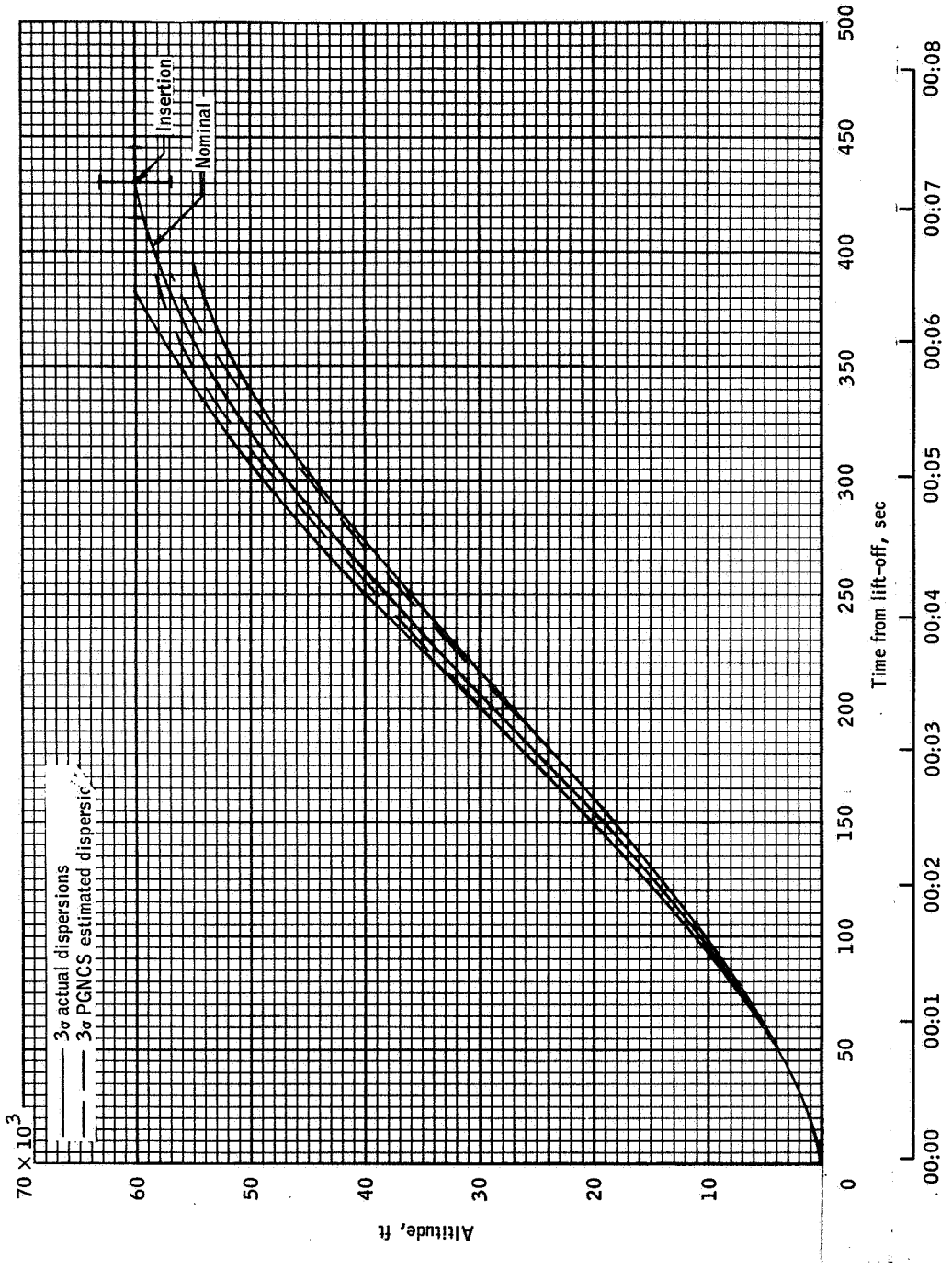

Figure 1.- Dispersions in altitude.

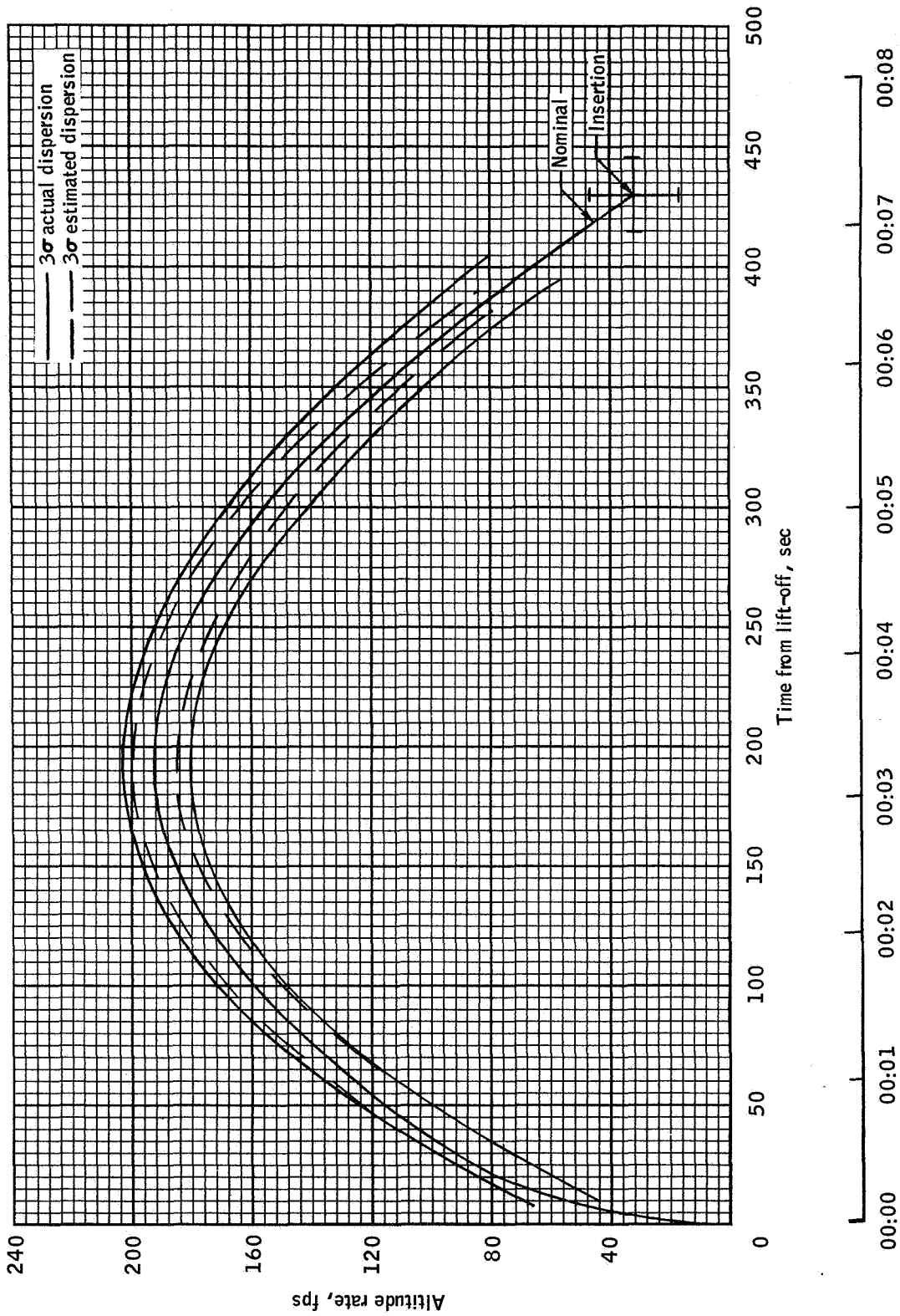

Figure 2.- Altitude rate dispersions.

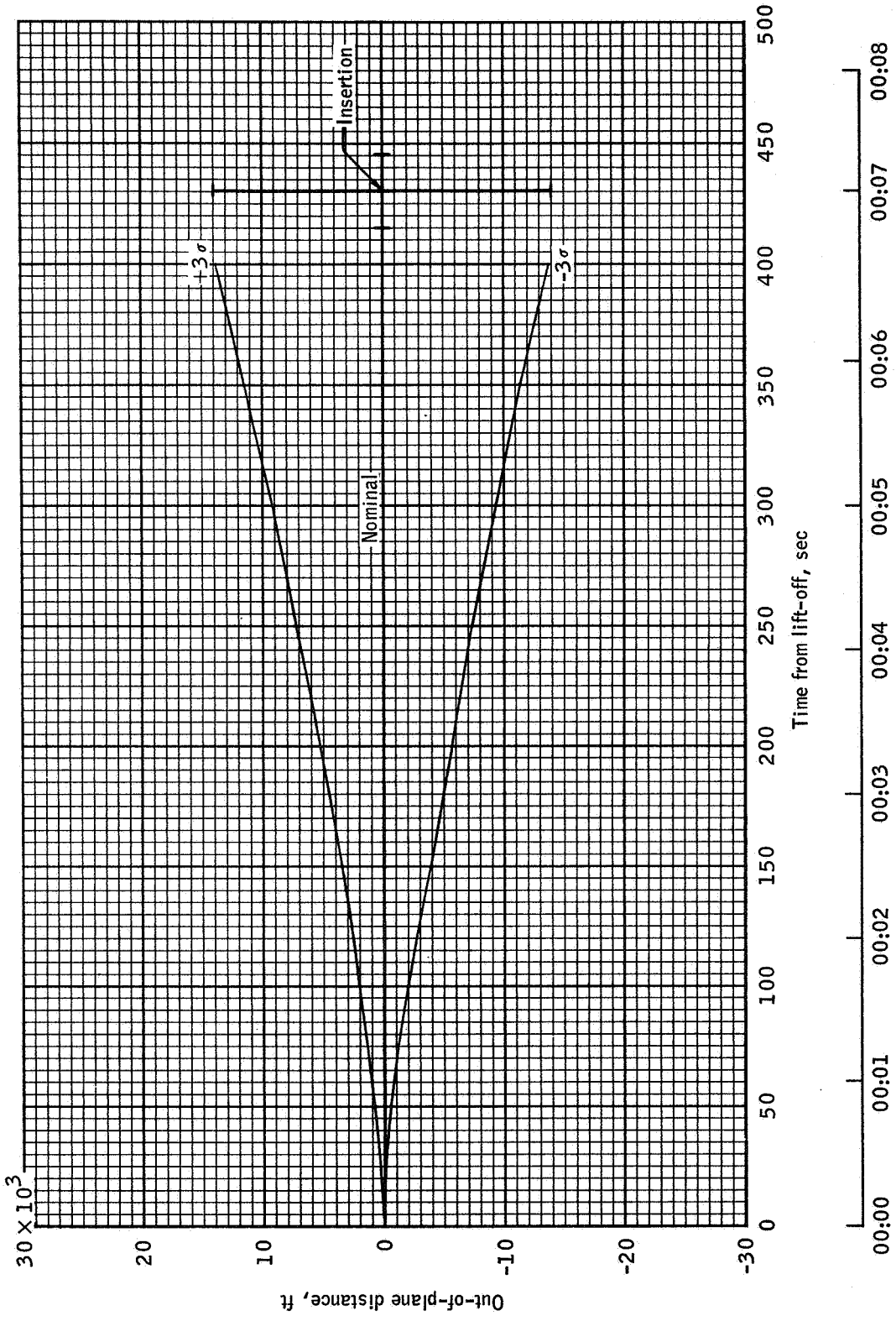

Figure 3.- Actual out-of-plane distance deviations.

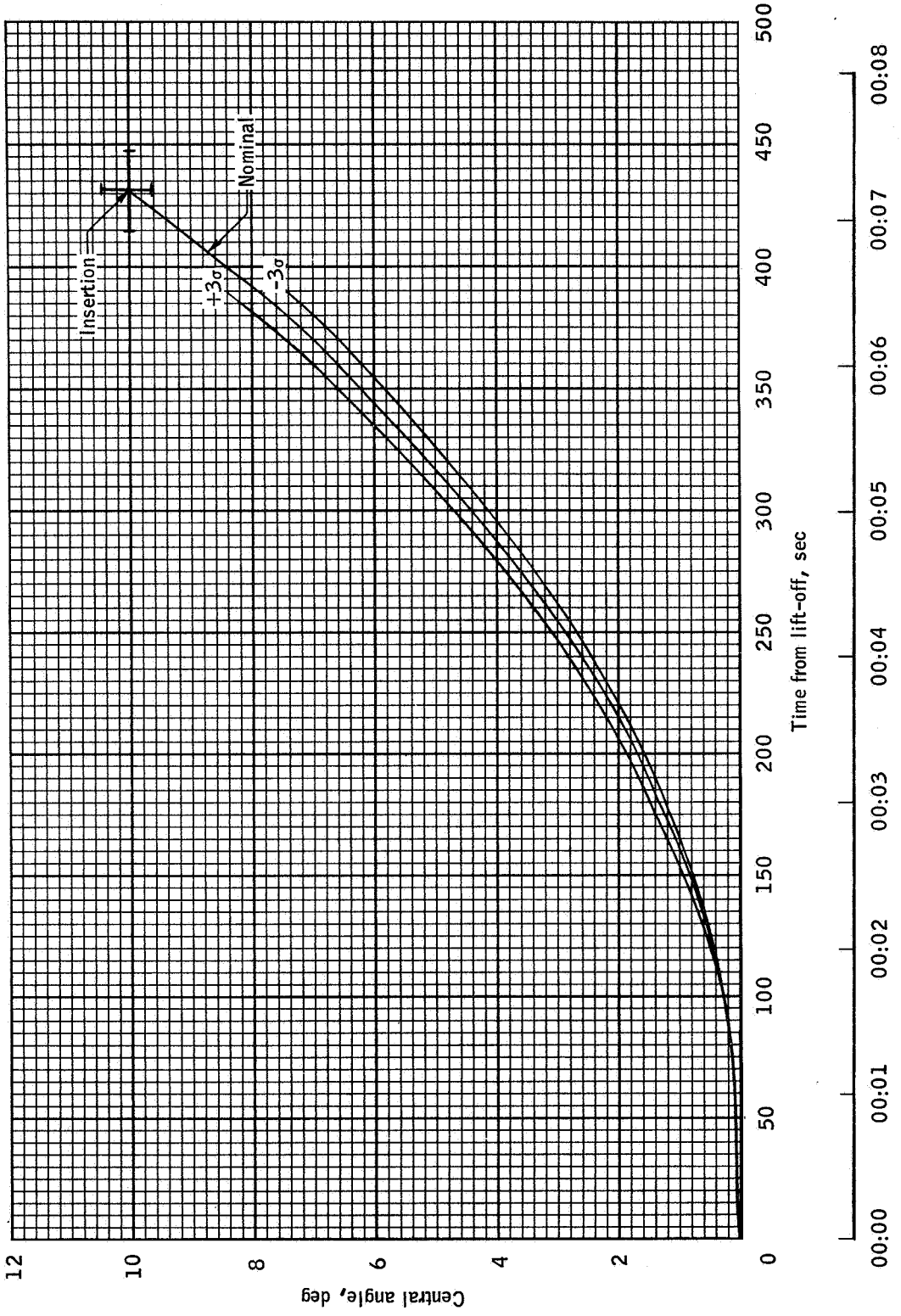

Figure 4.- Dispersions in the angle at center of moon between landing site and LM.

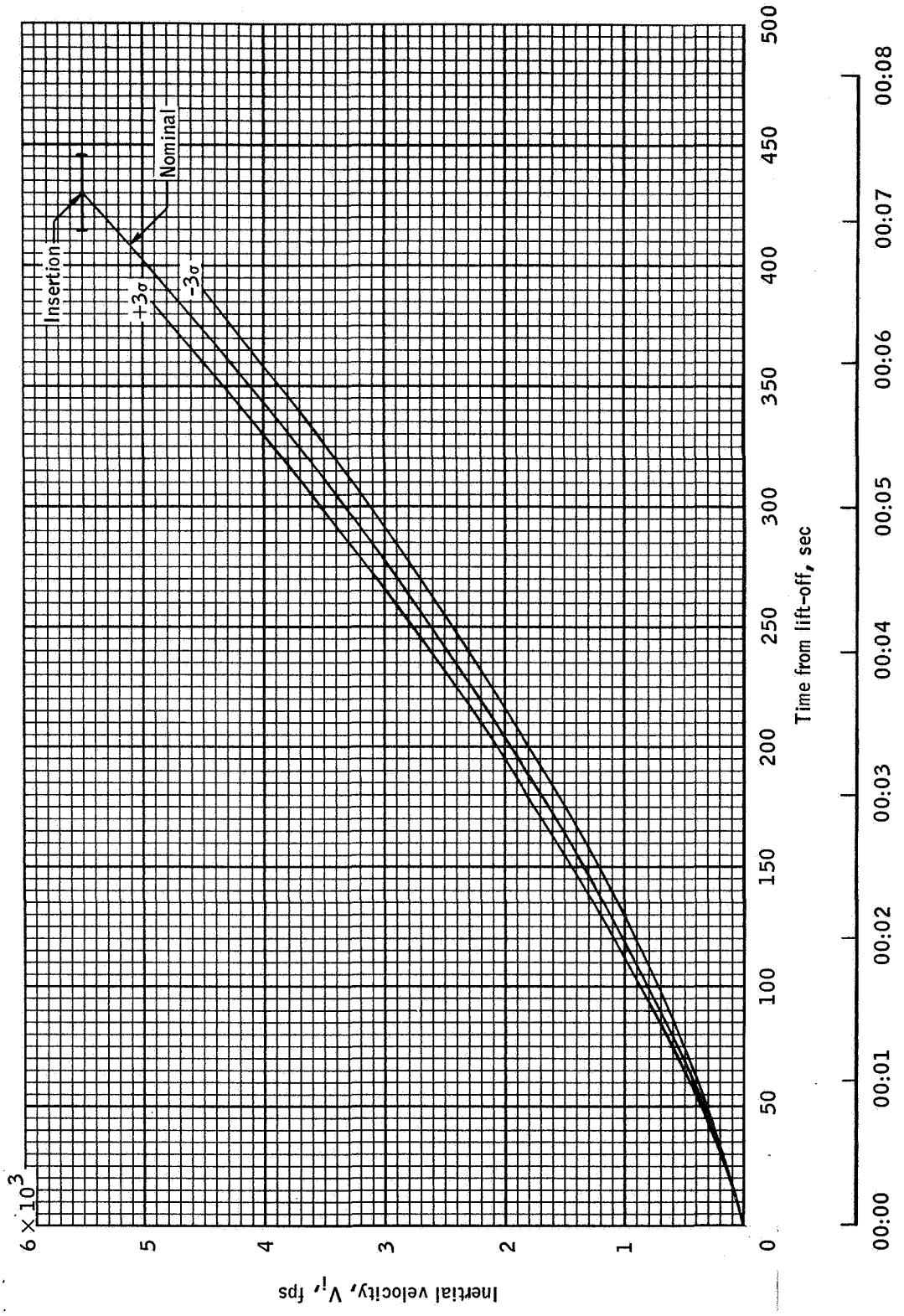

Figure 5.- Dispersions in actual inertial velocity.

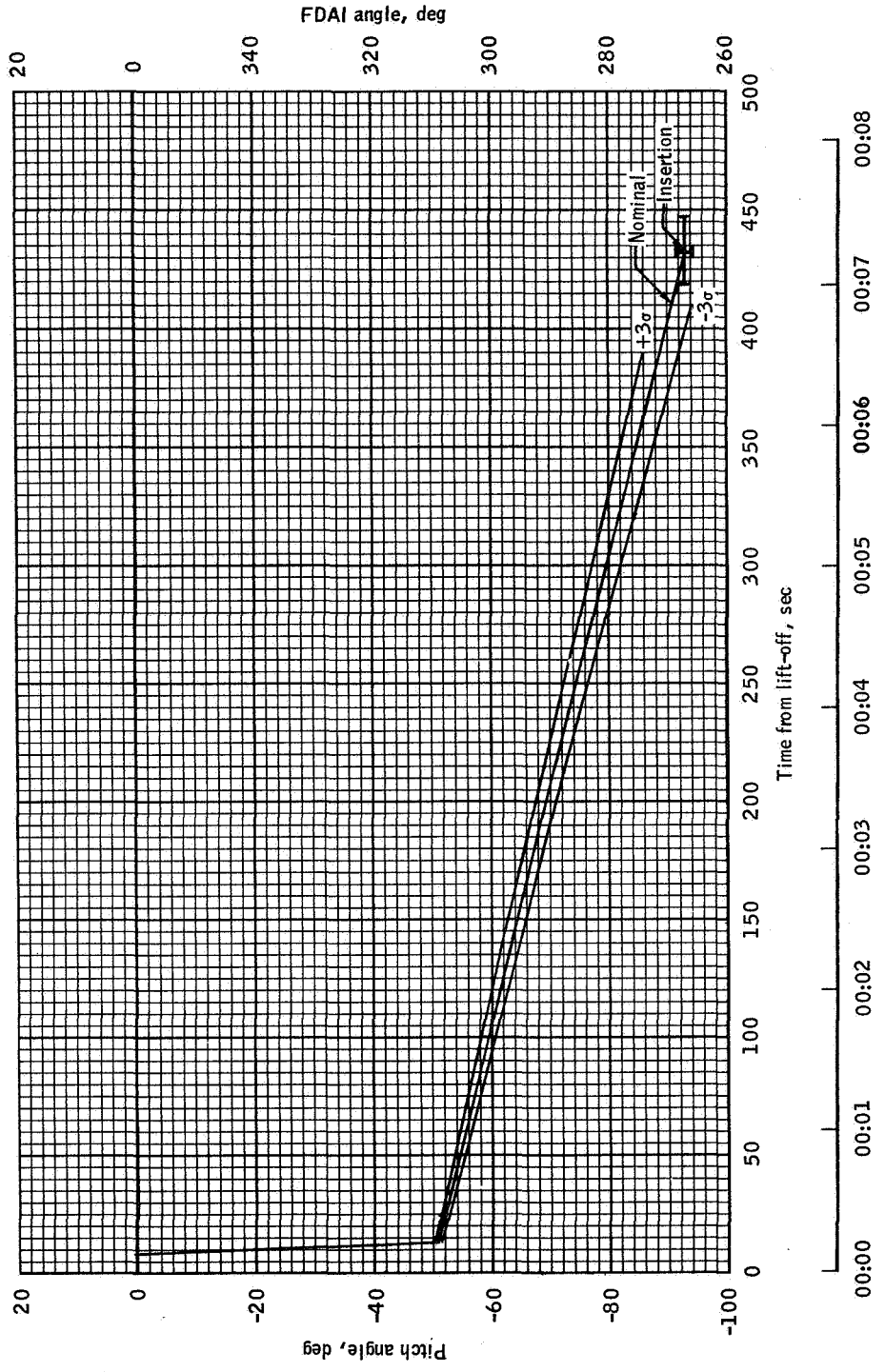

Figure 6.- Actual dispersions in pitch from local vertical.

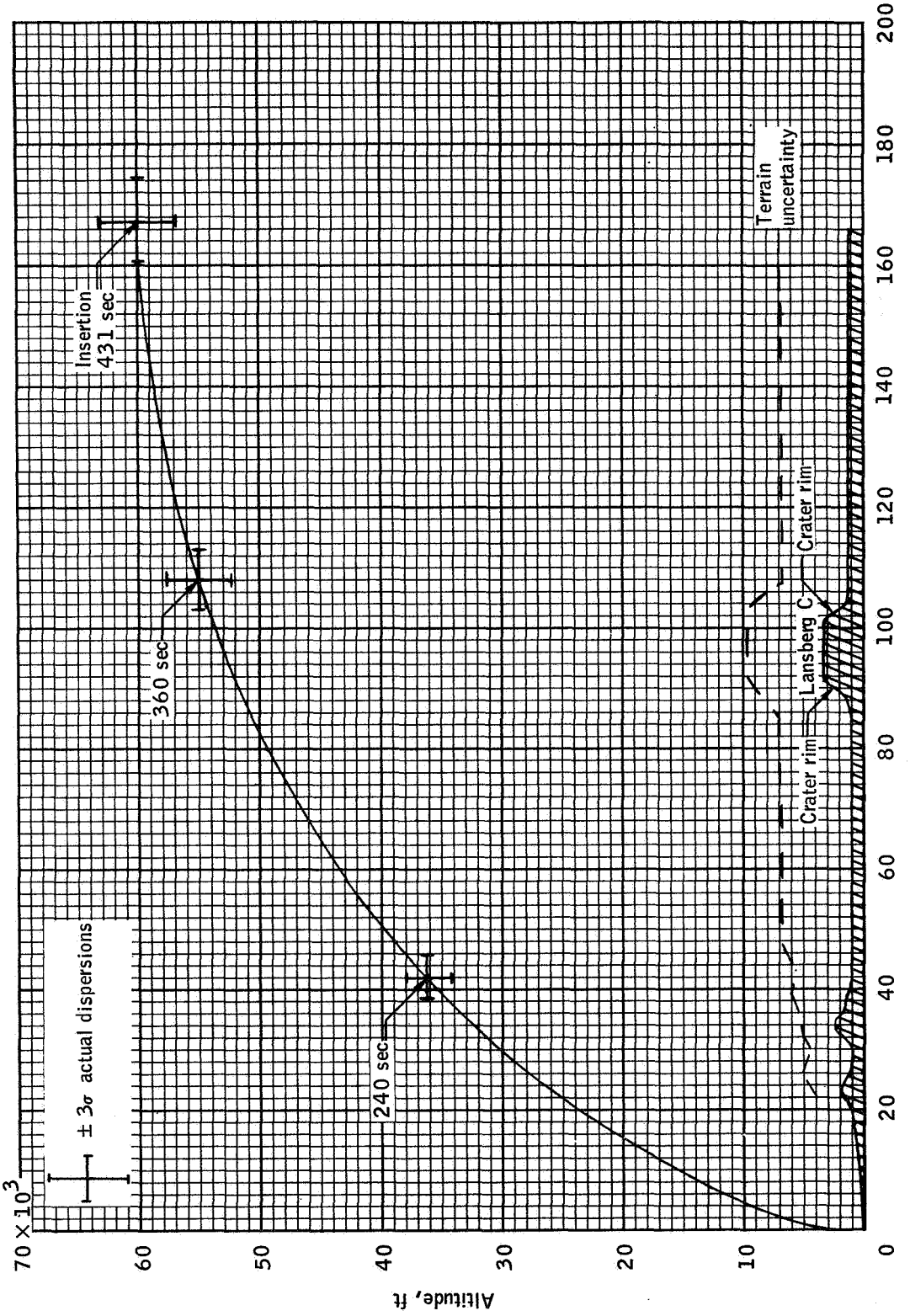

Figure 7.- Terrain clearance over highest elevations near lunar ascent groundtrack (site 2).

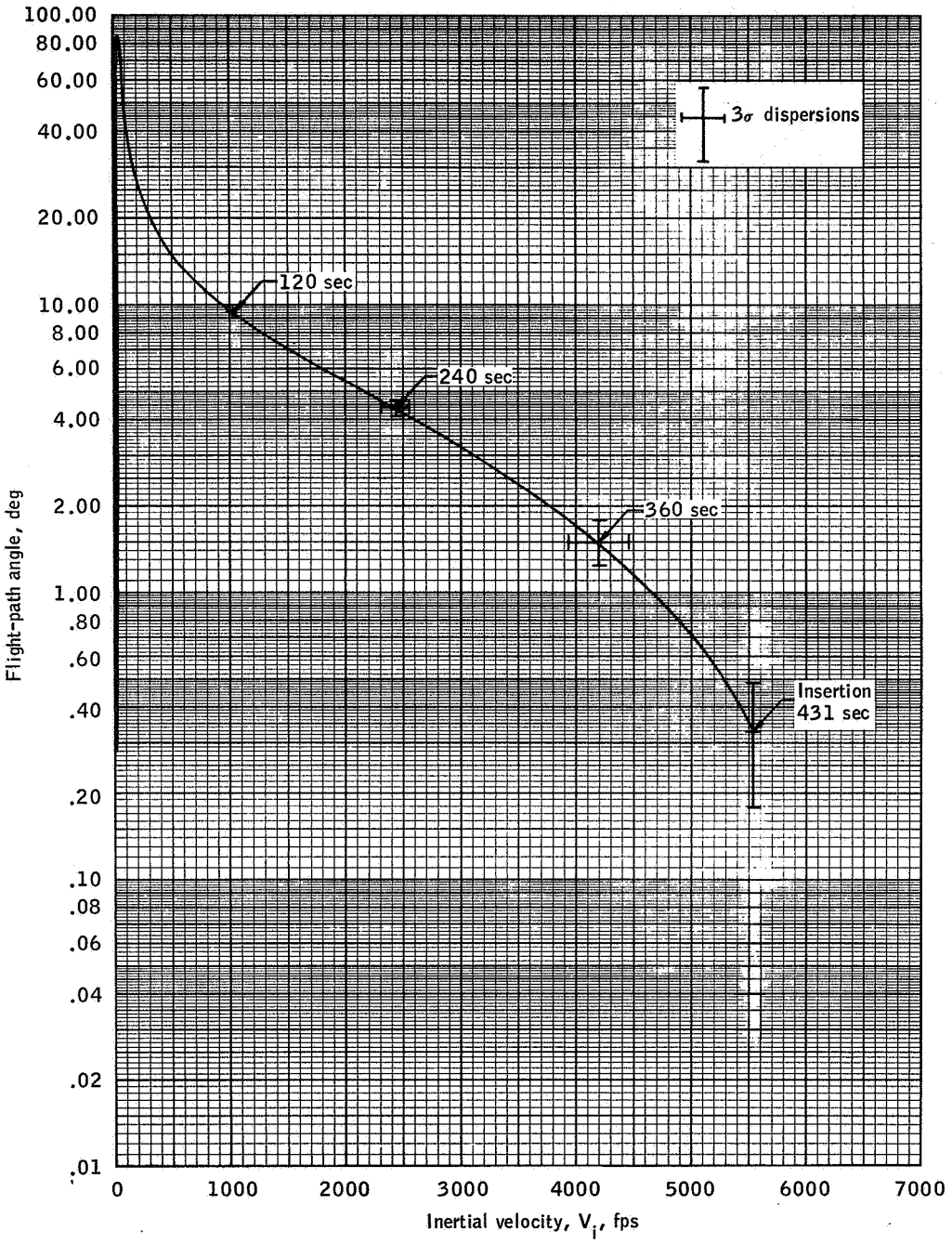

Figure 8.- Inertial velocity versus flight-path angle.

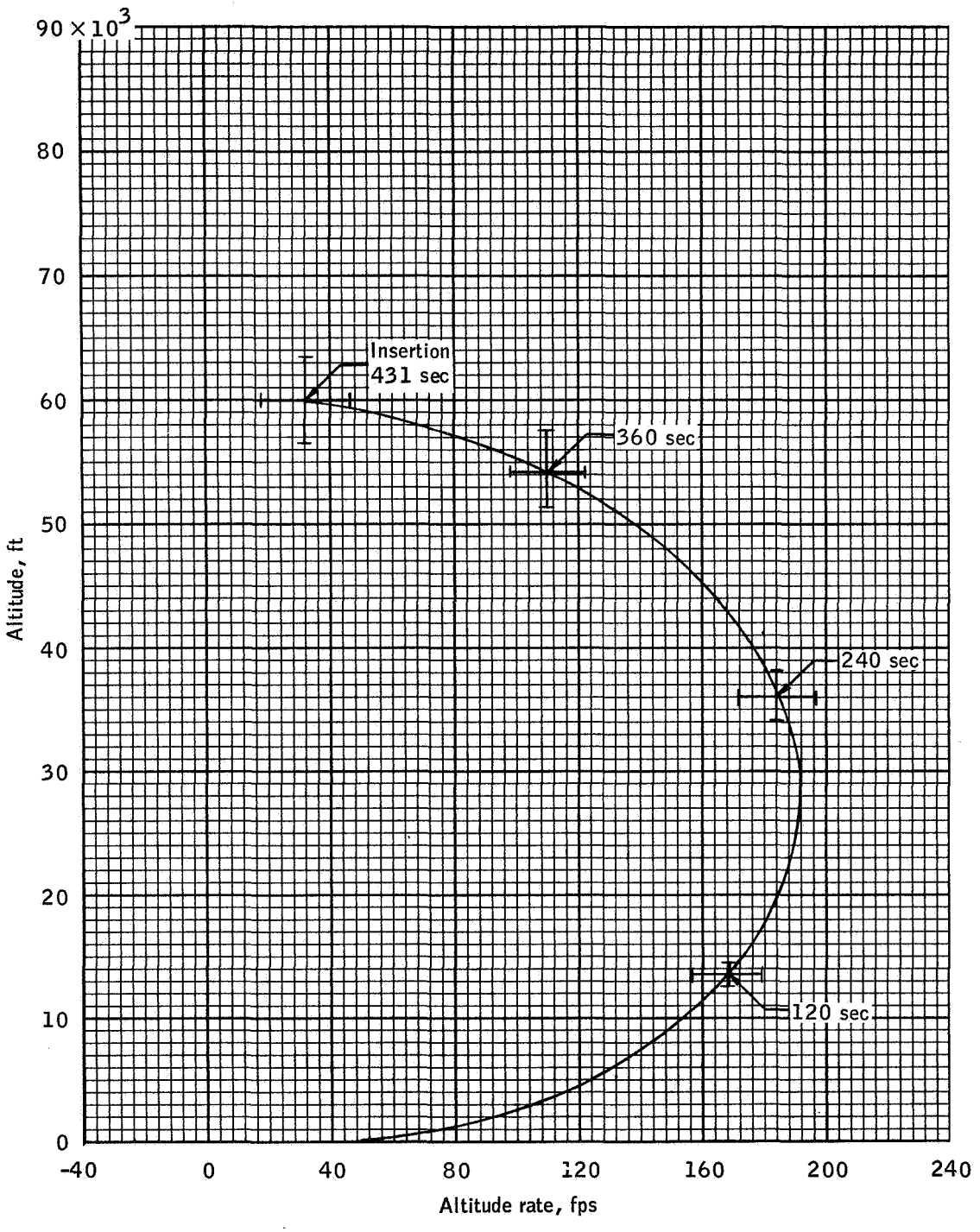

Figure 9.- Altitude versus altitude rate. (Actual)

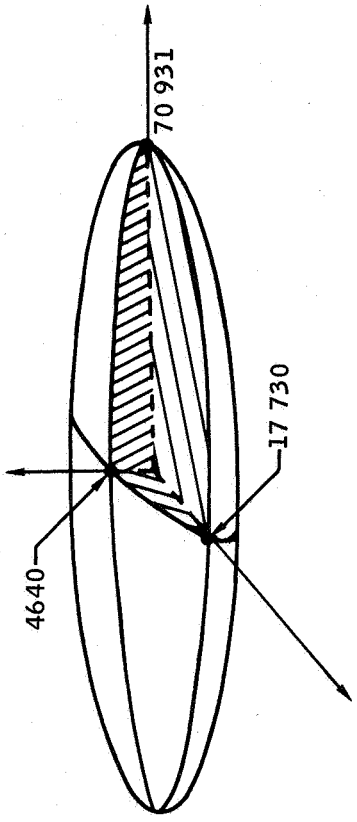

Figure 10.- 3σ position ellipsoid at t_{IG} + 460 seconds.

REFERENCES

1. Dvorkin, D.: Mission H-1 Lunar Orbit Covariance Matrices for CSM State Vector Updates Preceding CSM PC, LM INS, and TPI. MSC memo 69-FM46-311, October 6, 1969.

2. Williamson, J. B.: Navigation Update Accuracies for Targeting G Mission Lunar Ascent. MSC memo 69-FM46-96, April 9, 1969.

3. LMAB; LAB; and OMAB: Spacecraft Operational Trajectory for Mission H, Volume II - Operational Mission Profile Trajectory Parameters, Launched November 14, 1969. MSC IN 69-FM-242, September 15, 1969.

4. Clifford, J. B.: Implementation of the "R2" Potential Model Into the Apollo Guidance Computer. TRW IOC 5522.5-47, March 19, 1969.

5. Janak, P.: Polynominal Curve Fit Equations for Characteristic Curves of LM-6/APS Performance Prediction. TRW IOC 69.4353.2-74, August 25, 1969.

6. CSM/LM Spacecraft Operational Data Book, Volume II - LM Data Book. September 15, 1969.

7. Nolley, J.: Error Source Data for Dispersion Analysis. MSC IN 68-FM-297, December 13, 1968. Including Revision 1, February 14, 1969.

8. CSM/LM Spacecraft Operational Data Book, Volume III - Mass Properties.

9. LAB: Apollo 11 (Mission G) Dispersion Analysis Volume IV Descent and Ascent Dispersion Analyses Part 2 - Lunar Ascent. MSC IN 69-FM-166, June 20, 1969.

10. MIT GSOP R-567, Section 5, April 1969.

11. Schock, V. G., Jr.: Engineering Description of TAPP VIA. TRW Note 68-FMT-647, June 13, 1968.